

## CHAPTER 3

### MEASUREMENT OF THE HENRY NUMBER

#### 3.1. Introduction.

Numerous papers have been published dealing with theoretical and experimental aspects of the solubility of gases in liquids. A survey of relevant literature in this field is given in a number of excellent reviews [72-78]. Therefore, we refer to the voluminous review by Battino and Clever [72] and, of more recent date, to the reviews by Wilhelm and Battino [73] and Wilhelm, Battino and Wilcock [74]. The reviews by Wilhelm et al. [73,74] give a large number of reliable data on the solubility of gases in organic solvents and in water. In these reviews, however, neither the apparatus nor the method used is described.

In view of the permanent need for reliable engineering data on the solubility of gases in complicated mixtures, we have developed a relatively simple and inexpensive method by which it is possible to obtain accurate values of the Henry number.

We needed the values of the Henry number of slightly water-soluble gases at a total pressure of about 1 bar in the temperature range 20 - 60 °C to calculate the diffusion coefficients [79], as will be described in Chapter 4. Our method can be classified into the category of manometric-volumetric methods.

Most of the methods from this category are based on a saturation technique where the Henry number is calculated from the volume of gas absorbed into a sample of degassed liquid. This amount of gas is determined at known temperature and pressure. The technique we used is based on the so-called extraction method [72]. Under well-defined conditions of temperature and pressure, the liquid is saturated with gas. After saturation, a known mass of the liquid is drawn from the saturation apparatus and placed in the extraction device. In this apparatus the sample is evacuated and the gas is desorbed from the liquid.

After desorption, the volume of gas is determined in a gas burette at known temperature and pressure. From these experimental results, the Henry number is calculated.

In this chapter we shall describe the method and the apparatus used.

Further it will be shown that a good agreement is obtained between our and other authors' experimental values of the Henry number for the hydrogen-water system.

#### 3.2. Theory.

When a liquid is saturated with a slightly soluble gas A at temperature  $T_s$  and pressure  $p_s$ , the concentration of the gas in the liquid can be expressed by:

$$C_{AS} = p_{As} H_e / (\tilde{R}T_s) \quad (3-1)$$

so the Henry number is obtained from:

$$H_e = C_{AS} \tilde{R}T_s / p_{As} \quad (3-2)$$

If a mass of liquid  $m$ , saturated at  $T_s$  and  $p_s$ , is placed in the extraction apparatus and desorbed, the amount of gas A in the burette is given by:

$$N_A = p_{Ab} V_b / (\tilde{R}T_b) \quad (3-3)$$

From eqn (3-3), the solubility of gas A can be calculated if the density  $\rho_s$  of the saturated liquid at the saturation temperature  $T_s$  is known:

$$C_{AS} = \rho_s N_A / m \quad (3-4)$$

Substitution of eqn (3-4) into eqn (3-2) gives the Henry number:

$$H_e = (\rho_s \tilde{R} T_s / m) (N_A / p_{As}) \quad (3-5)$$

After discussion of the equipment, the Henry number will be expressed in physical quantities which can be measured directly.

### 3.3. Equipment.

An outline drawing of the saturation apparatus is given in Fig. 3.1. The apparatus consists of two bubble columns placed one above the other. Both columns  $A_1$  and  $B_1$  are thermostatted. Water from the thermostat enters the bubble columns at  $H_1$  and leaves them at  $I_1$ . Bubble column  $B_1$  is almost completely filled with the same degassed solvent as used in  $A_1$ . In column  $B_1$  the gas is saturated with vapour at the same temperature and at a small overpressure. Column  $A_1$  contains the solution to be examined. The temperature of the solution can be read by means of thermometer  $C_1$  which is situated in the liquid. The accuracy of this reading is  $\pm 0.1$  K. The gas enters the saturation apparatus at  $G_1$  and leaves it at  $F_1$ . The pressure drop owing to the gas flow in the pipe to the vent is measured by means of the manometer  $E_1$ . Each bubble column is provided with a porous glass plate as sparger to achieve a uniform distribution of gas in the column. Column  $A_1$  can be shut off by means of the stopcocks  $K_1$  and  $L_1$ . In this saturation apparatus, the gas is continuously led through the bubble columns and sluiced into the atmosphere. In Fig. 3.2. an outline drawing of the extraction apparatus is given. The apparatus consists of a gas burette  $A_2$ , a sample holder  $B_2$  and a mercury reservoir  $C_2$ , which are all made of glass. The sample holder  $B_2$  and the reservoir  $C_2$  are connected by a vacuum hose  $D_2$ . This vacuum hose and part of the reservoir and sample holder are filled with mercury. The length of the vacuum hose is about 1 m. The gas burette  $A_2$  is thermostatted and is provided with a measuring scale, which must be calibrated beforehand at a certain temperature.

We calibrated the gas burette with mercury at 20 °C. On both sides, the gas burette is provided with stopcocks,  $E_2$  and  $F_2$ . The length of the burette is about 20 cm; its diameter is about 3 mm. The capacity of the burette used in the present experiments is about 1.5 cm<sup>3</sup>. It is of course possible to use a burette with a different capacity, to be able to determine a different range of gas solubilities while avoiding too small or too large amounts of liquid sample. The gas burette  $A_2$  is placed upon the sample holder  $B_2$  by means of a ground joint  $K_2$ . The sample holder  $B_2$  has a diameter of about 4 cm and is about 9 cm long. Its capacity is about 100 cm<sup>3</sup>. In the experiments with water as solvent we used about 50 cm<sup>3</sup> of water for each experiment.

The ground joint  $K_2$  is mounted with the smaller opening at the top to prevent that gas bubbles cannot escape from  $B_2$ . The reservoir  $C_2$  has a diameter of about 3.5 cm and is about 5.5 cm long. Its capacity is about 50 cm<sup>3</sup>. The reservoir  $C_2$  should contain enough mercury, so that it still contains some mercury when the liquid sample is brought into the gas burette  $A_2$  up to stopcock  $E_2$  by moving the reservoir  $C_2$  upwards. Furthermore,  $C_2$  should have sufficient capacity to collect all the mercury flowing from the sample holder  $B_2$  into the reservoir  $C_2$ , when the liquid sample is evacuated and the gas is desorbed. The mercury in  $C_2$  is blanketed with a small layer of water.

### 3.4. Procedure.

Before we started the desorption experiments, the gas burette was calibrated at 20 °C with mercury. The volume of gas in the burette as a function of the reading is given by:

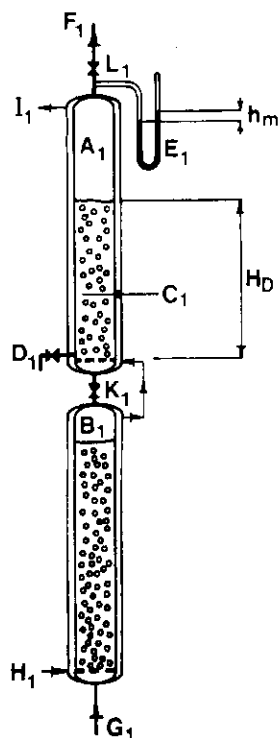


Fig. 3.1. Saturation apparatus.  
 A<sub>1</sub> bubble column with sample  
 B<sub>1</sub> bubble column  
 C<sub>1</sub> thermometer  
 D<sub>1</sub> outlet of column A<sub>1</sub>  
 E<sub>1</sub> manometer  
 F<sub>1</sub> gas outlet  
 G<sub>1</sub> gas inlet  
 H<sub>1</sub> water from thermostat  
 I<sub>1</sub> water to thermostat  
 K<sub>1</sub> and L<sub>1</sub> stopcocks

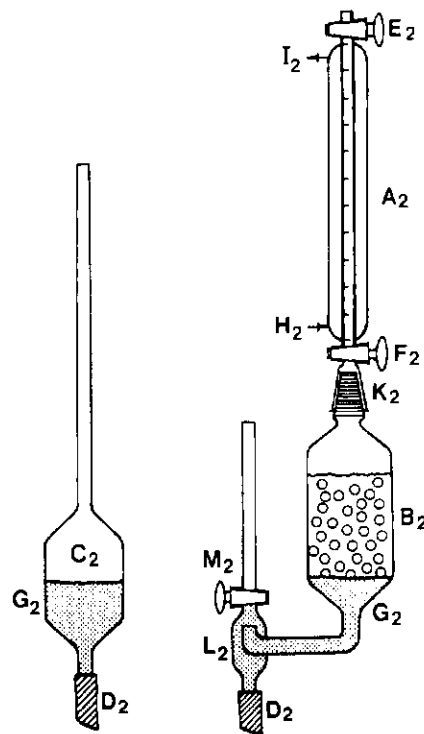


Fig. 3.2. Extraction apparatus.  
 A<sub>2</sub> gas burette  
 B<sub>2</sub> sample holder  
 C<sub>2</sub> mercury reservoir  
 D<sub>2</sub> vacuum hose  
 E<sub>2</sub> stopcock  
 F<sub>2</sub> stopcock  
 G<sub>2</sub> mercury  
 H<sub>2</sub> water from thermostat  
 I<sub>2</sub> water to thermostat  
 K<sub>2</sub> ground joint B 12  
 L<sub>2</sub> small vessel  
 M<sub>2</sub> stopcock

$$V_b = V_1 + V_2G \quad (3-6)$$

Before each set of experiments, the columns A<sub>1</sub> and B<sub>1</sub> of the saturation apparatus are filled with degassed solvent. The degassed solvent is saturated by a continuous flow of gas through the bubble columns. The rate of gas absorption is given by:

$$k_L a V_D (C_{As} - C_A(t)) = -V_L d(C_{As} - C_A(t))/dt \quad (3-7)$$

Integration of eqn (3-7) with the initial condition:

$$t = 0 \quad C_A = 0 \quad (3-8)$$

yields, after rearranging:

$$(C_{As} - C_A(t))/C_{As} = \exp(-k_L a V_D t / V_L) \quad (3-9)$$

The saturation time is then given by:

$$t = - \frac{\ln(1 - C_A(t)/C_{As})}{k_L a V_D / V_L} \quad (3-10)$$

The specific area is determined from:

$$a = 6 \epsilon_{av} / d_s \quad (3-11)$$

and

$$V_L / V_D = 1 - \epsilon_{av} = H_0 / H_D \quad (3-12)$$

Substitution of eqns (3-11) and (3-12) into eqn (3-10) gives:

$$t = - \frac{\ln(1 - C_A(t)/C_{As})}{6 k_L \epsilon_{av} / ((1 - \epsilon_{av}) d_s)} \quad (3-13)$$

Both gas holdup and mean bubble diameter are estimated visually. The liquid-film mass transfer coefficient can be estimated from a relation given by Calderbank [37]:

$$k_L Sc^{1/2} = 0.42 (\Delta \rho r_{LG} / \rho_s^2)^{1/3} \quad \text{for } d_s > 2.5 \text{ mm} \quad (3-14a)$$

and

$$k_L Sc^{2/3} = 0.31 (\Delta \rho r_{LG} / \rho_s^2)^{1/3} \quad \text{for } d_s < 2.5 \text{ mm} \quad (3-14b)$$

These equations give a reliable estimation of the time required to saturate the solvent B with gas A in a bubble column.

The saturation pressure of the gas is the barometric pressure plus the excess pressure in the column  $A_1$  indicated by manometer  $E_1$  plus the average static pressure of the saturated liquid in the column minus the vapour pressure of the solvent at the given saturation temperature:

$$P_{As} = b_0 + h_m \rho_s g - P_{Vs} + \frac{1}{2} H_0 \rho_s g \quad (3-15)$$

The manometer used to measure the excess pressure of column  $A_1$  is filled with the same solvent as that in which the Henry number is to be determined. A sample of liquid is now taken from column  $A_1$ .

This is done by opening stopcock  $D_1$  and bringing the sample into a vessel of about 50 cm<sup>3</sup>. This vessel is drawn in Fig. 3.3. It is a double-wall vessel of glass in which space  $B_3$  is evacuated.

When space  $A_3$  is filled with saturated liquid, the vessel is closed and the mass of the vessel with the liquid,  $m_1$ , is determined.

The saturated liquid is now brought into the extraction apparatus. Tube  $D_3$  of the small vessel is placed just above the mercury level and a small overpressure of the gas whose Henry number is to be determined is imposed upon tube  $C_3$ . Owing to the small overpressure, the liquid flows into the sample holder  $B_2$ . When the sample holder has been filled, the gas burette  $A_2$  is placed on  $B_2$  and the mass  $m_2$  of the vessel with the remaining liquid is determined. The mass of the liquid sample in the extraction apparatus is now given by:

$$m = m_1 - m_2 \quad (3-16)$$

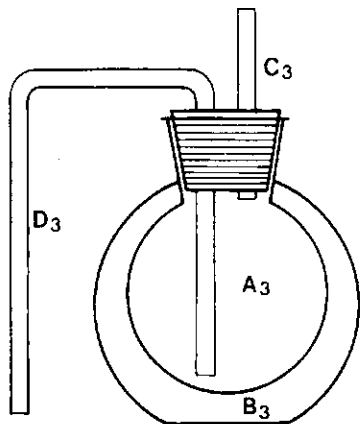


Fig. 3.3. Apparatus to determine the mass of the liquid in the sample holder.  
 A<sub>3</sub> vessel of about 50 cm<sup>3</sup>                      C<sub>3</sub> gas inlet  
 B<sub>3</sub> evacuated space                                      D<sub>3</sub> liquid outlet

When the gas burette is placed on the sample holder B<sub>2</sub> of Fig. 3.2., the liquid level of the sample is brought just beneath stopcock E<sub>2</sub> at the top of the measuring scale by moving the mercury reservoir C<sub>2</sub> upwards. The reservoir C<sub>2</sub> is fixed and stopcock E<sub>2</sub> is closed. The liquid is now thermostatted at 20 °C. Owing to the vapour pressure of the solvent at 20 °C and the possible change in volume of the solvent caused by the temperature difference between saturation temperature and desorption temperature, a small difference may arise between the pressure in the burette and the atmospheric pressure. Therefore, stopcock E<sub>2</sub> is opened to equalize the pressure in the burette A<sub>2</sub> and the barometric pressure. The volume of gas between the solvent level in the burette and stopcock E<sub>2</sub> consists of air and vapour. The small amount of air is given by:

$$N_o = (b_o - p_{vb})V_o / (\tilde{R}T_b) \quad (3-17)$$

in which:

$$V_o = V_1 + V_2G_o \quad (3-18)$$

After the scale reading has been noted down, reservoir C<sub>2</sub> is moved downwards and/or the sample holder B<sub>2</sub> upwards until the liquid level is at stopcock F<sub>2</sub>. This stopcock is now closed and the sample holder B<sub>2</sub> is moved further upwards. Gas is desorbed from the liquid and collected under stopcock F<sub>2</sub>. When the sample holder has been vibrated for a while, the sample holder is moved downwards and fixed at a certain height. Stopcock F<sub>2</sub> is opened and the desorbed gas is added to the gas in the burette A<sub>2</sub>. The procedure described above is repeated until no more gas is desorbed from the liquid. This can be checked by marking the liquid level in the gas burette each time when the sample holder B<sub>2</sub> is fixed at the same height.

When the desorption procedure has been finished, stopcock F<sub>2</sub> is opened and the gas is led into the gas burette while the reservoir C<sub>2</sub> is moved upwards until the mercury levels in the reservoir C<sub>2</sub> and the sample holder B<sub>2</sub> are at the same height.

The amount of gas in the gas burette after desorption is given by:

$$N_e = p_b V_e / (\tilde{R}T_b) \quad (3-19)$$

in which:

$$V_e = V_1 + V_2 G_e \quad (3-20)$$

Now,  $p_b$  is the total pressure of the gas in the burette and equals the barometric pressure minus the pressure which is due to the static height of the solvent:

$$p_b = b_e - h_b \rho_b g \quad (3-21)$$

The total amount of gas is the sum of the amount of air initially present in the burette, the amount of vapour and the amount of gas of which the Henry number is to be determined:

$$N_e = N_o + N_v + N_A \quad (3-22)$$

So, the amount of gas A desorbed from the known mass of liquid is calculated from:

$$N_A = N_e - N_o - N_v \quad (3-23)$$

The amount of vapour is given by:

$$N_v = p_{vb} V_e / (\tilde{R} T_b) \quad (3-24)$$

Substitution of eqns (3-17), (3-19), (3-21) and (3-24) into eqn (3-23) yields:

$$N_A = (b_e - h_b \rho_b g) V_e / (\tilde{R} T_b) - (b_o - p_{vb}) V_o / (\tilde{R} T_b) - p_{vb} V_e / (\tilde{R} T_b) \quad (3-25)$$

Substitution of eqns (3-25), (3-15) and (3-16) into eqn (3-5) gives for the Henry number:

$$H_e = \frac{T_s \rho_s}{T_b (m_1 - m_2)} \frac{(b_e - h_b \rho_b g - p_{vb}) V_e - (b_o - p_{vb}) V_o}{b_o + h_m \rho_s g - p_{vs} + \frac{1}{2} H_0 \rho_s g} \quad (3-26)$$

From this equation the Henry number can be calculated. All the quantities on the right-hand side of this equation can be measured directly.

### 3.5. Results.

We have determined experimentally the Henry numbers of three hydrogen-liquid systems viz.:

- hydrogen - water;
- hydrogen - aqueous hydroxylamine solution;
- hydrogen - aqueous 3-pentanone solution.

#### 3.5.1. Water.

The Henry number of hydrogen in water has been determined experimentally at about 1 bar total pressure in the temperature range 20-70 °C. Experiments were carried out with hydrogen of ultra-high purity, obtained from Matheson, claiming 99.999 % purity. The experimental results are listed in Table 3.1. It is obvious that our results deviate most at a temperature of 60 °C. The maximum deviation is about 7 per cent. The mean deviations of our results from the values reported by Himmelblau [75], Wilhelm et al. [74] and by Perry et al. [80] are 2.2, 2.3 and 1.9 per cent respectively. The overall-mean deviation of our results with these tabulated values is about 2 per cent. In general, our results show good agreement with values of the Henry number reported by others.

Table 3.1. Experimental results of the determination of the Henry number of hydrogen in water at about 1 bar total pressure.

T/°C	He 10 <sup>2</sup>	$\sigma_{\text{He}}$ 10 <sup>2</sup>	number of experiments
20	1.95	0.02	12
30	1.88	0.01	12
40	1.85	0.02	11
50	1.85	0.02	10
60	1.86	0.02	12
70	1.87	0.03	5

In Table 3.2. a comparison between literature data and our results is made.

Table 3.2. Henry numbers of hydrogen in water at about 1 bar total pressure. Comparison between our experimental results and values from literature data.

	He 10 <sup>2</sup>				
	20 °C	30 °C	40 °C	50 °C	60 °C
This work	1.95	1.88	1.85	1.85	1.86
Wilhelm et al. [74]	1.94	1.90	1.89	1.91	1.97
Himmelblau [75]	1.92	1.89	1.89	1.92	1.99
Perry [80]	1.95	1.89	1.89	1.90	1.95

### 3.5.2. Aqueous hydroxylamine solution.

In the range 20-70 °C we have determined the Henry number of hydrogen in an aqueous hydroxylamine solution.

This solution contained 30 mol m<sup>-3</sup> hydroxylamine phosphate and 300 mol m<sup>-3</sup> potassium dihydrogen phosphate. The experimentally determined values of the Henry number are summarized in Table 3.3. The experiments were performed at a total pressure of about 1 bar.

Table 3.3. Experimental results of the determination of the Henry number of hydrogen in an aqueous hydroxylamine solution at a total pressure of about 1 bar.

T/°C	He 10 <sup>2</sup>	$\sigma_{\text{He}}$ 10 <sup>2</sup>	number of experiments	$\rho_s / (\text{kg m}^{-3})$
20	1.68	0.04	11	1029
30	1.62	0.03	10	1027
40	1.61	0.03	10	1023
50	1.65	0.03	10	1019
60	1.80	0.03	14	1015
70	1.99	0.04	10	1008

From the literature no information is available about  $H_e$  values of the solution mentioned in Table 3.3. Comparison of the experimental results of Table 3.3. with those of pure water shows that the Henry number for the electrolyte solution is smaller except at 70 °C.

### 3.5.3. Aqueous solution of 3-pentanone.

Further we have determined the value of the Henry number of hydrogen in an aqueous 3-pentanone solution containing 100 mol m<sup>-3</sup> 3-pentanone. The experiments were performed at 30 °C. For the Henry number we found a value of  $1.8 \cdot 10^{-2}$ . The standard deviation was  $0.1 \cdot 10^{-2}$  for 9 experiments. Comparison of the Henry number of hydrogen in a mixture of 3-pentanone and water with the value for water gives a somewhat lower value for the mixture.

### 3.6. Conclusions.

It has been shown in this chapter that application of the described extraction method leads to reliable values of the Henry numbers of slightly soluble gases in liquids at about 1 bar total pressure, provided that:

- the liquid in the bubble column has been saturated completely;
- the partial pressure of the solvent component(s) is known and is not too high;
- the static height in the bubble column is relatively small, e.g. 20 cm liquid;
- the bubble column contents are well-mixed;
- the volume of air above the liquid in the gas burette before desorption is as small as possible.

This extraction method can be used to generate reliable engineering data. Further we have shown that in the range 20-60 °C our experimental results for the solubility of hydrogen in water deviate by about 2-6 per cent from literature data [74,75,80].

Addition of electrolytes or an organic solute to water decreased the solubility of hydrogen.

### 3.7. Discussion.

A disadvantage of the above-described method is the long time it takes to saturate the liquid with gas and to desorb the gas from the sample. The initial idea of the above-described equipment is from Kusters [81]. During fruitful discussions about the subject of measuring solubilities of slightly soluble gases in liquids Kusters proposed to modify the equipment as used by Ben Naim and Baer [82].

They proposed equipment for quick determination of the solubility of a gas in a liquid by means of the saturation method. The modification is that the apparatus is not only used to saturate the liquid but also to evacuate the liquid to make it solute free. Further, the dissolution vessel is not completely filled with degassed solvent so that a stream of liquid from the central capillary travels through the gas phase.

The very rapid mass transfer occurring at this procedure can be explained by means of the penetration theory.

In Fig. 3.4a., a stream of liquid for gas absorption is represented. Owing to the very short exposure of the liquid to the gas phase, the depth of penetration of the gas is small with respect to the radius of the liquid stream. The gas penetrates the liquid stream only during the contact time, after which the stream is well mixed up in the bulk of the liquid.

By this mixing the absorbed gas is homogenized in the liquid and new gas is again absorbed into the liquid.

The penetration depth of the gas into the liquid is given by:



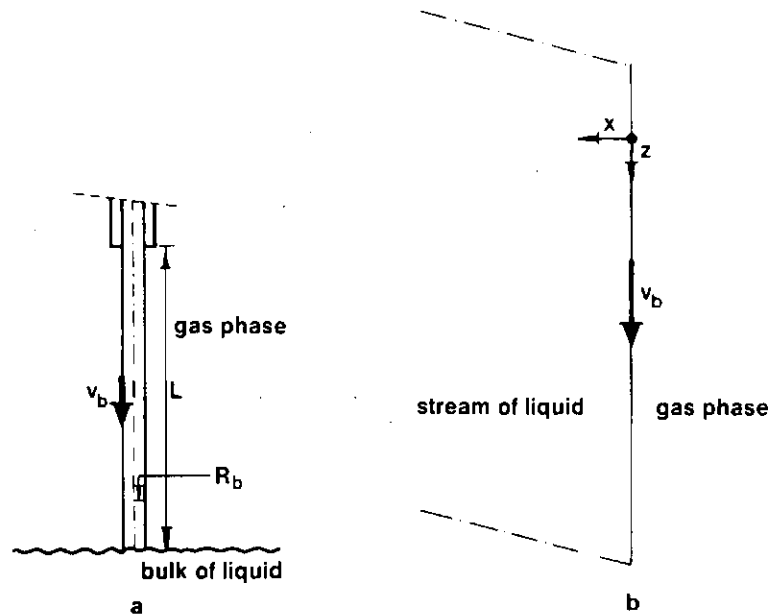


Figure 3.4. Representation of the stream of liquid.

$$\delta = 4(DL/v_b)^{\frac{1}{2}} = 4(Dt_c)^{\frac{1}{2}} \ll R_b \quad (3-27)$$

where  $t_c$  is the contact time  $L/v_b$ .  
The penetration theory can now be applied if:

$$Dt_c/R_b^2 \equiv Fo \ll 1/16 \quad (3-28)$$

If the depth of penetration is small compared with the radius of the liquid stream, the surface of the cylinder can be considered a plane surface. The representation of this surface is given in Fig. 3.4b. A simplified relation for the concentration of gas in the liquid stream is given by:

$$C_A(x,z)/C_{AS} = 1 - \operatorname{erf} (x/(4Dz/v_b)^{\frac{1}{2}}) \quad (3-29)$$

so that the molar flux is:

$$J_A(t) = (D/(\pi t))^{\frac{1}{2}}(C_{AS} - C_{Ab}) \quad (3-30)$$

When applying the penetration theory the mass transfer coefficient is given by:

$$k_L(t) = (D/(\pi t))^{\frac{1}{2}} \quad (3-31)$$

The mean mass transfer coefficient during the contact time  $t_c$  is:

$$\bar{k}_L = 2(D/(\pi t_c))^{\frac{1}{2}} \quad (3-32)$$

It is obvious that high values of the mass transfer coefficient are obtained if the contact time is very short.

On the analogy of eqn (3-10), the saturation time is calculated from:

$$t = - \frac{\ln(1 - C_A(t)/C_{As})}{\bar{k}_L a_L} \quad (3-33)$$

The specific interfacial area  $a_L$  is determined from:

$$a_L = 2\pi R_b L / V_L \quad (3-34)$$

whereas the mean liquid film mass transfer coefficient is calculated from eqn (3-32).

Ben Naim and Baer reported a 99 % saturation within 2-3 minutes. From eqn (3-33) it is found that for this case  $\bar{k}_L a_L$  lies between  $2.6 \cdot 10^{-2}$  and  $3.8 \cdot 10^{-2} \text{ s}^{-1}$ .

To have the same rate of gas absorption in a bubble column ( $k_L = 10^{-4} \text{ m s}^{-1}$ ), a specific interfacial area of about  $4 \cdot 10^2 \text{ m}^{-1}$  is required.

If  $d_s = 3 \text{ mm}$ , the gas holdup in the bubble column must be as high as 0.2.

It is clear that the use of a stream of liquid in a gas-liquid system has some advantages:

- desorption and absorption processes are performed in one vessel;
- the gas absorption rate is high;
- there is no unnecessary loss of gas.

CHAPTER 4

MEASUREMENT OF DIFFUSION COEFFICIENTS

4.1. Introduction.

Since 1950, several techniques have been proposed for the measurement of the diffusion coefficients of slightly soluble gases in liquids. In some of these, diffusion coefficients are determined by means of the technique of the dissolving gas bubble, in which the volume of gas absorbed into the liquid is calculated from the decrease of bubble size with time. This method, referred to as the DBS-method, generally leads to unreliable results.

Epstein and Plesset [83] presented the mathematical solution of the diffusion problem of a gas bubble dissolving into an undersaturated solution.

They assumed that:

- in a stagnant liquid the centre of the gas bubble is at rest at the origin of a spherical polar coordinate system;
- only diffusive mass transport occurs in a radial direction.

For the change of bubble radius with time, they derived that:

$$\frac{dR}{dt} = - \frac{D_{AB}(c_R - c_\infty)\tilde{R}T}{p_R R} \left( 1 + \frac{R}{(\pi D_{AB} t)^{\frac{1}{2}}} \right) \quad (4-1)$$

Since this theory, some papers have been published [84-87], which deal with the problem of mass transfer from a spherical bubble into an infinitely extended degassed liquid. In all of these papers, the authors simplified eqn (4-1) by neglecting the transient term, which leads to:

$$\frac{dR}{dt} = - \frac{D_{AB}(c_R - c_\infty)\tilde{R}T}{p_R R} \quad (4-2)$$

After integration of this equation, a linear relationship between  $R^2$  and  $t$  is obtained.

This result suggests that the diffusion coefficient can easily be calculated from the slope of this line. However, if measured values of  $R^2$  are plotted versus time, no straight line is found at all. This has been shown by Lieberman [84] and by Houghton et al. [85] and also in our laboratory.

In studying the problem of the experimental determination of the diffusion coefficient of slightly soluble gases into liquids, we were confronted with some major disadvantages, theoretical and experimental, of the DBS-method. Here they will be discussed briefly.

In the DBS-method it is assumed that the bubble surface moves in a radial direction. This forced convection influences the concentration gradient of the absorbed gas at the bubble surface in the liquid-phase so that the transient model valid for a constant bubble size may not be applied (Fig. 4.1a)

Moreover, it is experimentally impossible to hold a single bubble at rest in an infinite liquid medium without further provisions. To fix the gas bubble, it was attached to a horizontal or vertical plane surface [86,87].

As a consequence, the assumption of mass transfer into an infinite medium around the whole sphere is questionable. For this reason, Lieberman [84] suggested a correction of the measured diffusion coefficient by a factor  $\ln 2$ . However, in that case the bubble remained spherical with a point of contact between the sphere and the plane surface (Fig. 4.1b).

This correction was introduced to take into account the decreased mass transfer owing to the presence of an impermeable medium on one side of the bubble.

However, generally there is not one point of contact but a contact area between the sphere and the plane surface. Therefore, Manley [85] has introduced a correction for the presence of this contact area, taking into account

the contact angle e.g. between water and perspex. Further, we have to note that the centre of a gas bubble attached to a surface moves towards this surface if the radius is reduced by gas absorption from the gas bubble.

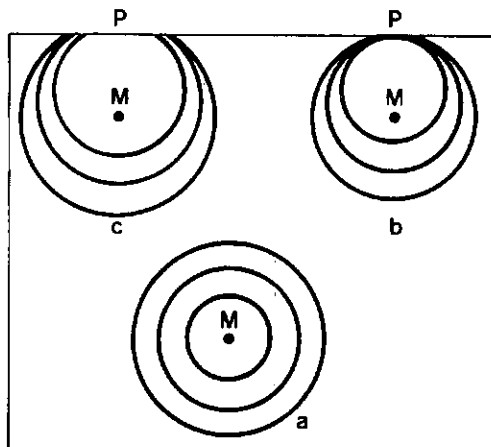


Fig. 4.1. DBS-method; bubble behaviour during absorption.  
a: the centre is fixed at M (hypothetical case)  
b and c: the centre moves along MP (real case)

Consequently, the centre of the gas bubble moves through the liquid phase so that the transport of the gas into the liquid phase will in part be convective (Fig. 4.1b. and 4.1c.).

Summarizing, we must conclude that with the DBS-method the mass transfer is not adequately described by eqn (4-1) and that the diffusion coefficient measured according to this method will be unreliable; this method will generally result in too high values of the diffusion coefficient. Therefore, we have developed the CBS-method, according to which the diffusion coefficient can be determined from the volume of gas added per unit of time to a gas bubble fixed at the tip of the needle of a syringe, to compensate for gas absorption to such an extent that the bubble diameter remains constant. In this case the mass transfer from the bubble can be calculated using the well-known equation for the unsteady radial mass transfer from a sphere of constant diameter in an infinitely extended stagnant medium.

#### 4.2. Theory.

Fig. 4.2. represents a gas bubble fixed at the tip of a needle ground in the shape of a truncated cone. The centre of the gas bubble coincides with the hypothetical top of this cone.

For unsteady diffusion of a gas A across an interface from a sphere into a stagnant solvent B, the equation of continuity for spherical coordinates leads to:

$$\frac{\partial c_A(r,t)}{\partial t} = D_{AB} \frac{1}{r^2} \frac{\partial}{\partial r} \left( r^2 \frac{\partial c_A(r,t)}{\partial r} \right) \quad (4-3)$$

Boundary and initial conditions for this problem are:

$$r = R \quad c_A(R,t) = c_R \quad \text{for } t > 0 \quad (4-4)$$

$$r \rightarrow \infty \quad c_A(r \rightarrow \infty, t) = c_\infty \quad \text{for } t > 0 \quad (4-5)$$

$$t = 0 \quad c_A(r,0) = c_\infty \quad \text{for } r > R \quad (4-6)$$

With these conditions, the following solution is found:

$$c_A(r,t) = c_\infty + (c_R - c_\infty)(R/r) \operatorname{erfc}(z) \quad (4-7)$$

with

$$z = (r - R)/\{2(D_{AB}t)^{1/2}\} \quad (4-8)$$

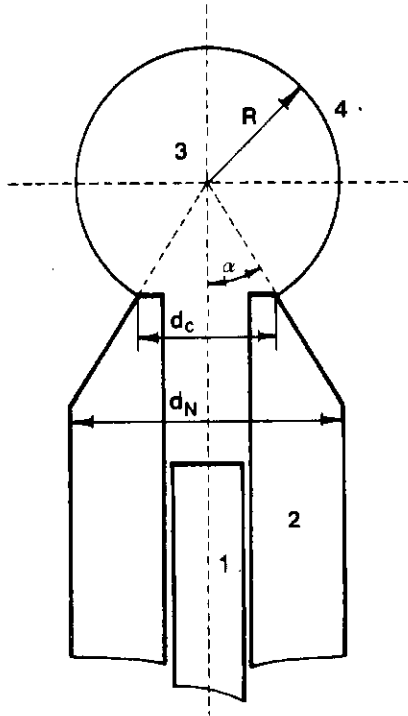


Fig. 4.2. Representation of the fixed gas bubble.  
1. plunger; 2. needle; 3. gas bubble; 4. liquid.

The molar flux of the gas at any time and any distance, is given by:

$$J_A(r,t) = -D_{AB} \frac{\partial c_A(r,t)}{\partial r} = (c_R - c_\infty)D_{AB} \left\{ \frac{R}{r^2} \operatorname{erfc}(z) + \frac{R}{r} \frac{1}{(\pi D_{AB}t)^{1/2}} e^{-z^2} \right\} \quad (4-9)$$

From this equation, the molar flux at the gas-liquid interface can be derived:

$$J_A(R,t) = \frac{D_{AB}(c_R - c_\infty)}{R} \left( 1 + \frac{R}{(\pi D_{AB}t)^{1/2}} \right) \quad (4-10)$$

So, the rate of absorption from a sphere into a stagnant liquid is:

$$\phi_A(t) = 4\pi R D_{AB} (c_R - c_\infty) \left(1 + R/(\pi D_{AB} t)^{\frac{1}{2}}\right) \quad (4-11)$$

However, not the entire surface of the gas bubble is available for mass transfer, because of the presence of the cone-shaped needle. The area of this blocked segment of the sphere is given by:

$$A_c = 2\pi R^2 \int_0^\alpha \sin(\theta) d\theta = 2\pi R^2 (1 - \cos(\alpha)) \quad (4-12)$$

This means that the fraction  $\gamma$  of the bubble surface area available for mass transfer is:

$$\gamma = 1 - 2\pi R^2 (1 - \cos(\alpha)) / (4\pi R^2) = \frac{1}{2}(1 + \cos(\alpha)) \quad (4-13)$$

Considering this result, the rate of absorption across the interface of a bubble on a needle is:

$$\phi_A^*(t) = \frac{1}{2}(1 + \cos(\alpha)) 4\pi R D_{AB} (c_R - c_\infty) \left(1 + R/(\pi D_{AB} t)^{\frac{1}{2}}\right) \quad (4-14)$$

The total number of moles A absorbed from the gas bubble into the liquid at time  $t = t'$ , can be found by simply integrating this equation:

$$N_A^*(t') = 2(1 + \cos(\alpha)) R^3 (c_R - c_\infty) \left(\pi D_{AB} t' / R^2 + 2(\pi D_{AB} t' / R^2)^{\frac{1}{2}}\right) \quad (4-15)$$

Furthermore, the concentration of the gas in the liquid at the interface can be given, applying Henry's law:

$$c_R = H_e p_R / (\tilde{R}T) \quad (4-16)$$

Assuming the gas to be ideal, the volume of gas A absorbed is calculated from:

$$V_A^*(t') = N_A^*(t') \tilde{R}T / p_R \quad (4-17)$$

From eqns (4-15), (4-16) and (4-17) it follows:

$$V_A^*(t') = 2(1 + \cos(\alpha)) R^3 H_e \left(\pi D_{AB} t' / R^2 + 2(\pi D_{AB} t' / R^2)^{\frac{1}{2}}\right) \quad (4-18)$$

assuming  $c_\infty = 0$ . From eqn (4-18) we find that the volume of the absorbed gas A is independent of the partial pressure  $p_R$  of the gas A in the bubble, provided that  $H_e$  is independent of  $p_R$ .

Equation (4-18) can be rearranged to fit a straight line through the origin:

$$\left\{ \left( \frac{V_A^*(t')}{2(1 + \cos(\alpha)) R^3 H_e} + 1 \right)^{\frac{1}{2}} - 1 \right\}^2 = \frac{\pi D_{AB}}{R^2} t' \quad (4-19)$$

The diffusion coefficient is now found from the slope  $m$  of the straight line obtained by plotting the left-hand side of this equation against  $t'$ :

$$D_{AB} = m R^2 / \pi \quad (4-20)$$

It should be pointed out that in this technique no arbitrary bubble diameter can be used. The diameter is determined by the top angle  $\alpha$  and the diameter  $d_c$  of the truncated cone:

$$d = d_c / \sin(\alpha) \quad (4-21)$$

Only in this case is the requirement fulfilled that the centre of the gas bubble should coincide with the hypothetical top of the truncated cone.

#### 4.3. Equipment.

An outline drawing of the apparatus and its provisions is given in Fig. 4.3.

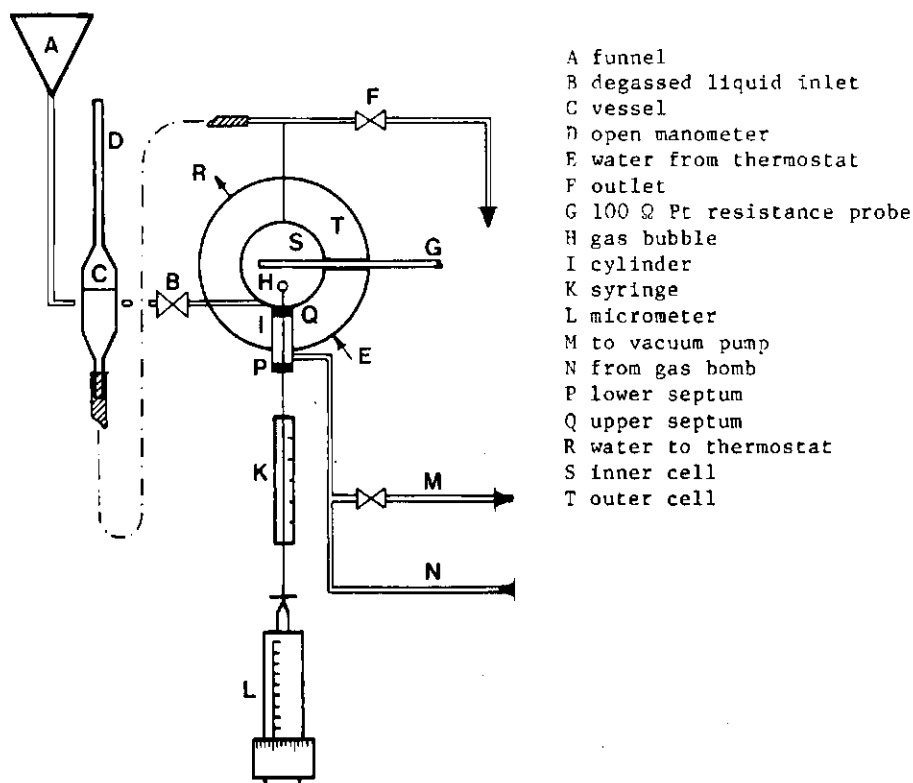


Fig. 4.3. Outline drawing of the apparatus and its provisions.

The diffusion cell consists of two small cylindrical tubes placed concentrically one inside the other. The cell is of one piece of material. The inner cylinder S has an inside diameter of 15 mm and an outside diameter of 20 mm. Its length is 15 mm. Both ends of this inner cell are closed by a circular perspex plate which is pressed against an O-ring in the flange, to avoid any leakage from the inner cell. The outer cylinder T has an inside diameter of 50 mm and an outside diameter of 70 mm. It is 30 mm long and both ends are closed by a circular perspex plate of the same diameter. The temperature of the liquid in the inner cell is controlled by means of thermostatted water flowing through the space enclosed by both cylinders. This temperature is read with a HP-2802A thermometer equipped with a 100 Ω Pt-resistance probe, type 18643 A. Accuracy of this apparatus is within  $\pm 0.5$  K. The resolution is 0.01 K. The probe G is placed inside the inner cell. Temperature fluctuations during experiments were less than 0.04 K. Degassed liquid can flow into and out of the cell through inlet B and outlet F respectively. Both inlet and outlet can be shut off by means of a stopcock, placed as close as possible upon the apparatus itself. The inlet of this cell is connected to a small funnel A at a somewhat higher level. The outlet is connected to an open manometer D to permit of adjusting the pressure of the gas in the bubble H to the barometric pressure, so that there will be no pressure drop and, consequently, no leakage along the plunger into the needle of the syringe K. This is done by moving vessel C in a vertical direction so

that the liquid level in vessel C is at the same height as the top of the gas bubble.

At the bottom of the cell, a little stainless steel cylinder I with an inner diameter of 6 mm has been placed, which is on each side closed by means of a septum. This construction is represented in Fig. 4.4.

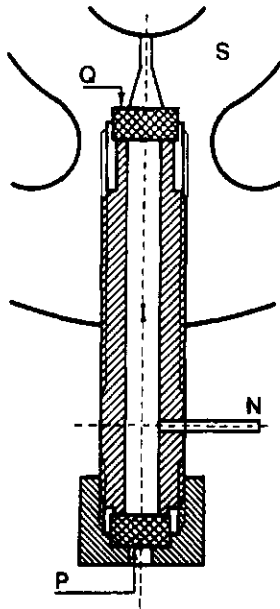


Fig. 4.4. Construction of the gas cylinder I.  
S diffusion cell; I gas cylinder; N from gas bomb; Q upper septum;  
P lower septum.

Further, we used an optical system for accurate measurement of the bubble diameter. The bubble and the tip of the needle are projected on a screen, with a magnification of about 100 times as shown in Fig. 4.5.

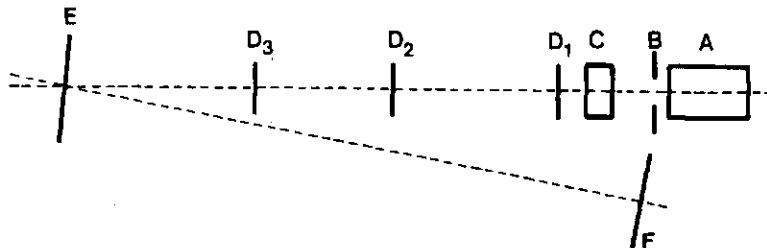


Fig. 4.5. Optical system.  
A source of light  
B diaphragm  
C diffusion apparatus  
D<sub>1</sub>, D<sub>2</sub> and D<sub>3</sub> lenses  
E mirror  
F screen

The apparatus is placed between a source of light with a diaphragm and some lenses. With the diaphragm, the intensity of the light is decreased to prevent local heating of the liquid in the inner cell, so that no free convection of the liquid near the gas bubble can occur. The picture of the needle with the



bubble is reflected by a mirror to form an enlarged image on the screen just beside the diffusion apparatus. For this reason, much care was taken to make sure that all perspex and/or glass plates of the diffusion cell were plane parallel.

#### 4.4. Procedure.

For each experiment, the inner cell is filled with degassed liquid after having been flushed with about 150 ml of the liquid. Then, the tip of the needle is pricked through the lower septum P and the cylinder I is evacuated. After vacuum has been reached, this cylinder is filled with gas of which the diffusion coefficient has to be determined. This procedure is repeated five times. By pulling down the plunger of the syringe K, the needle is filled with gas. After the needle has been pricked through the upper septum Q into the degassed liquid, the syringe is fixed and the thimble of the micrometer L is turned to move the plunger upwards to form a bubble H of required diameter. The bubble size is checked on the screen. The required bubble diameter  $d^0$  on the screen is obtained from the values of the angle  $\alpha$  and the diameter  $d_c^0$  of the truncated cone, measured on the screen:

$$d^0 = d_c^0 / \sin(\alpha) \quad (4-22)$$

The real bubble diameter is calculated from:

$$d = d^0 d_N / d_N^0 \quad (4-23)$$

where  $d_N / d_N^0$  gives the ratio between the diameters of the real needle and its image on the screen.

The thimble of the micrometer is turned manually so that on the screen the required diameter is obtained. The micrometer reading is noted down. During the next eleven minutes, the gas is continuously supplied so that in spite of the gas absorption the bubble diameter remains accurately constant, and the micrometer reading is noted down every 60 seconds.

To simplify this procedure, the picture of the bubble is projected on a sheet with a circle of diameter  $d^0$ . The total volume  $V_A^*(t')$  of gas absorbed at  $t = t'$  can now be calculated by multiplying the displacement of the micrometer from  $t = 0$  to  $t = t'$  by the volume displacement of the plunger per unit of displacement. After plotting values representing the left part of eqn (4-19) against the corresponding  $t'$  values, a straight line through the origin is obtained, the slope of which can be used to calculate the diffusion coefficient.

#### 4.5. Precautions.

We recognize that in performing these experiments, several possible error sources can occur. In the following, seven relevant error sources will be discussed shortly.

- The most important one is that of convection, both free and forced convection, by which the liquid in the inner cell will be no longer stagnant and eqn (4-3) will no longer stand.

Forced convection will be introduced by leakage of the inner cell.

Therefore, much care must be taken to ensure that both stopcocks and all junctions of the inner cell are leak-tight.

Free convection will be mainly introduced by differences in density of the liquid in the inner cell. If we ignore the differences in density which are due to differences in dissolved gas concentration, it is temperature differences which cause the free convection. In the method we used, these temperature differences can be initiated by the light needed to project an enlarged image of the bubble on the screen. When the intensity of this light is too high, local heating of the liquid in the inner cell will occur,

resulting in free convection of the liquid in the neighbourhood of the gas bubble. We found that even fluctuations in temperature as small as 0.2 K will lead to free convection. In our experiments, temperature fluctuations did not exceed 0.04 K. Grassmann [88] reported that free convection will not occur if  $Ra < 1800$ . This means that for our equipment, using water as a solvent in the temperature range 20 - 60 °C, the temperature differences must be smaller than 0.3 - 0.06 K respectively, taking the radius of the inner cell as the characteristic length.

- Much attention should be given to the fact that no leakage must occur along the plunger in the needle of the syringe. The syringe (SGE, type B), with a capacity of 1 or 5  $\mu$ l, cannot be guaranteed to be gas-tight. We therefore adjust the pressure of the gas in the gas bubble to the barometric pressure so that there will be no leakage along the plunger in the needle of the syringe owing to a pressure drop. We have found experimentally that leakage along the plunger can be neglected if the pressure drop along the plunger is smaller than 1000 Pa.
- The purity of the sample of gas of which the diffusion coefficient has to be determined must be ensured. For this reason, a closed system is used from which a sample of gas is drawn directly. This system is five times evacuated and filled with gas, to ensure that no impurities will be present. From the gas in this system, a sample is sucked into the needle of the syringe and placed directly into the degassed liquid. It is clear that when sucking up a gas sample with a syringe from an exterior gas bottle, the same purity can never be reached.
- Further, we used a very small overpressure in the gas bubble, to avoid aspiration of surrounding air along the plunger into the needle of the syringe. Therefore, the level of the liquid in vessel C is at the same height as the top of the gas bubble.
- The temperature of the gas in the bubble and in the needle must be the same as that of the liquid. It is therefore necessary for the part of the needle which is filled with gas to be totally within the cylinder I. This cylinder is surrounded by the water from the thermostat so that not only the gas in this cylinder but in particular that in the needle can be kept at the correct temperature.
- Further, we must recognize that the radius of curvature at the top of the gas bubble can be slightly different from that at the bottom. In this connection, it can be derived that:

$$1/R_B - 1/R_T = \rho_L g R / \sigma \quad (4-24)$$

The higher the value of the right-hand side of eqn (4-24), the more the shape of the gas bubble will differ from that of a sphere. Rearranging of the left-hand side of the eqn (4-24) leads to:

$$(R_T - R_B)R / (R_T R_B) = \Delta R / R = \rho_L g R^2 / \sigma \equiv Bo \quad (4-25)$$

In our experiments we used the restriction that:

$$Bo < 10^{-2} \quad (4-26)$$

from which it follows, with  $\rho_L = 10^3 \text{ kg m}^{-3}$ ,  $g = 9.81 \text{ m s}^{-2}$  and  $\sigma = 73 \cdot 10^{-3} \text{ N m}^{-1}$ , that:

$$R < 0.27 \cdot 10^{-3} \text{ m} \quad (4-27)$$

Therefore, size and shape of the needle are chosen so that for slightly soluble gases in water a bubble diameter of about 0.5 mm can be applied.

- Finally, the gas in the needle should be saturated with solvent vapour before the experiment starts. The time required to saturate the gas in the needle with solvent vapour can be calculated from:

$$t = \lambda^2/D_G \quad (4-28)$$

This can be obtained from the assumption that  $Fo \equiv D_G t/\lambda^2 = 1$  for the unsteady mass transfer into a semi-slab of length  $\lambda$ . For  $\lambda = 0.03$  m and  $D_G = 10^{-5} \text{ m}^2 \text{ s}^{-1}$ , we find  $t > 100$  s.

#### 4.6. Absorption of hydrogen in liquids.

Experiments were carried out with a number of gas-liquid systems:

- hydrogen-water in the temperature range 20 - 60 °C;
- hydrogen-aqueous electrolyte solution in the temperature range 30 - 60 °C;
- hydrogen-aqueous solution of 3-pentanone at 30 °C;
- hydrogen-1-propanol at 30 °C;
- hydrogen-n-heptane at 30 °C;
- hydrogen-aqueous polymer solution at 20 and 30 °C;
- helium-water in the temperature range 20 - 60 °C.

The syringes used were from Scientific Glass Engineering. The needles were ground in the shape of a truncated cone.

We used three syringes of 1  $\mu\text{l}$  and one syringe of 5  $\mu\text{l}$ . The sizes of the needles, the truncated cones and the enlarged pictures of the gas bubble on the screen are given in Table 4.1.

Table 4.1. Sizes of the needle and the bubble for different syringes used.

number		1	2	3	4
enlargement factor	$d_N^0/d_N$	106	108	104	104
needle diameter	$d_N$	0.52 mm	0.53 mm	0.53 mm	0.54 mm
	$d_N^0$	55 mm	57 mm	55 mm	56 mm
diameter of top of truncated cone	$d_c^0$	28 mm	24 mm	22 mm	38 mm
bubble diameter	$d$	0.49 mm	0.42 mm	0.40 mm	0.37 mm
	$d^0$	52 mm	46 mm	42 mm	38 mm
cone angle	$\alpha$	0.57 rad	0.55 rad	0.55 rad	$\pi/2$ rad
volume of syringe		1 $\mu\text{l}$	1 $\mu\text{l}$	1 $\mu\text{l}$	5 $\mu\text{l}$

Experiments were carried out with hydrogen and helium of research purity, obtained from Matheson, claiming 99.9999 % purity.

##### 4.6.1. Water.

Experiments were performed in the range 20 - 60 °C; results are given in Table 4.2. and Fig. 4.6.

The diffusion coefficients are calculated with the values of the Henry number from Chapter 3. Fig. 4.6. makes clear that our values are low compared with most of the values from the literature. In general, measurements are limited to room-temperatures. Only Wise et al. [87] and Ferrell and Himmelblau [89] have

performed experiments in a temperature range of 20 - 60 °C. Wise et al. used the DBS-method. In the introduction, we have already shown that values obtained with this method are not reliable because forced convection occurs. Ferrell and Himmelblau used the method of laminar dispersion in a capillary to determine the diffusion coefficient of hydrogen and helium in water. The disadvantage of this method is that both momentum and mass transfer occur and may interfere. Consequently, it can be expected that less accurate values of the diffusion coefficient will result. Recently, O'Brien and Hyslop [90] published data on the diffusion coefficient of hydrogen in water at 22 °C. They used an interferometric method to determine the diffusion coefficient in a stagnant liquid and took care that temperature fluctuations were within 0.03 K. Their value of  $3.0 \cdot 10^{-9} \text{ m}^2 \text{ s}^{-1}$  at 22 °C is in very good agreement with the data we obtained.

Table 4.2. Experimental values of the diffusion coefficient of hydrogen in water.

T/°C	D $10^9 / (\text{m}^2 \text{ s}^{-1})$	$\sigma_D$ $10^9 / (\text{m}^2 \text{ s}^{-1})$	number of experiments	$(D\eta_w \cdot 10^{14}/T)/(N/K)$
20	3.2	0.2	13	1.1
30	3.9	0.3	7	1.0
40	4.9	0.3	14	1.0
50	6.1	0.4	16	1.0
60	7.1	0.5	12	1.0

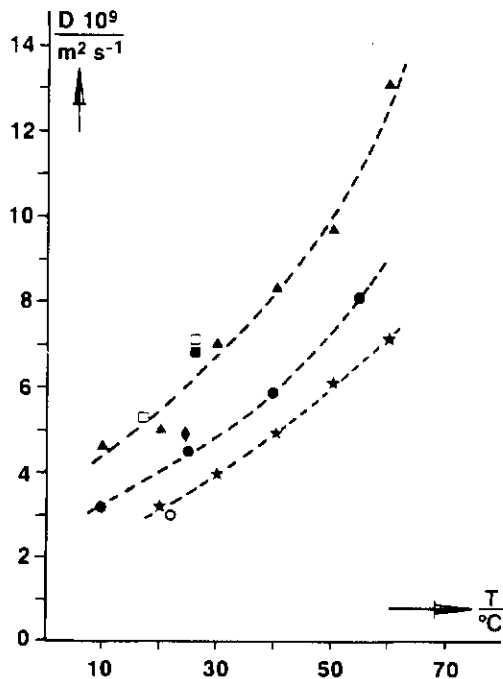


Fig. 4.6. Diffusion coefficient of hydrogen in water as a function of temperature.  $\blacklozenge$  Houghton [86],  $\square$  Davidson [91],  $\blacktriangle$  Wise [87],  $\blacksquare$  Davies [92],  $\bullet$  Ferrell [89],  $\circ$  O'Brien [90],  $\star$  present work.

#### 4.6.2. Aqueous hydroxylamine solution.

The electrolyte solution contains  $30 \text{ mol m}^{-3}$  hydroxylamine phosphate and  $300 \text{ mol m}^{-3}$  potassium dihydrogen phosphate and has a  $\text{pH} = 5$ . The experiments were performed in the range  $30 - 60 \text{ }^\circ\text{C}$ . The experimental results are given in Table 4.3. and in Fig. 4.7. The Henry numbers used in the calculations have been taken from the work described in Chapter 3.

From Fig. 4.7., it can be concluded that the values of the diffusion coefficient of hydrogen in the pure solvent are higher than those in the electrolyte solution. Because of the particular system, no information about the diffusion coefficient of hydrogen in the above-described solution is available from the literature.

The increase of the diffusion coefficient with temperature is comparable with that of the pure solvent.

Table 4.3. Experimental values of the diffusion coefficient of hydrogen in an electrolyte solution containing  $30 \text{ mol m}^{-3}$  hydroxylamine phosphate and  $300 \text{ mol m}^{-3}$  potassium dihydrogen phosphate.

T/ $^\circ\text{C}$	D $10^9/(\text{m}^2 \text{ s}^{-1})$	$\sigma_D 10^9/(\text{m}^2 \text{ s}^{-1})$	number of experiments
30	3.7	0.2	17
40	4.2	0.4	18
50	5.3	0.4	16
60	5.4	0.4	18

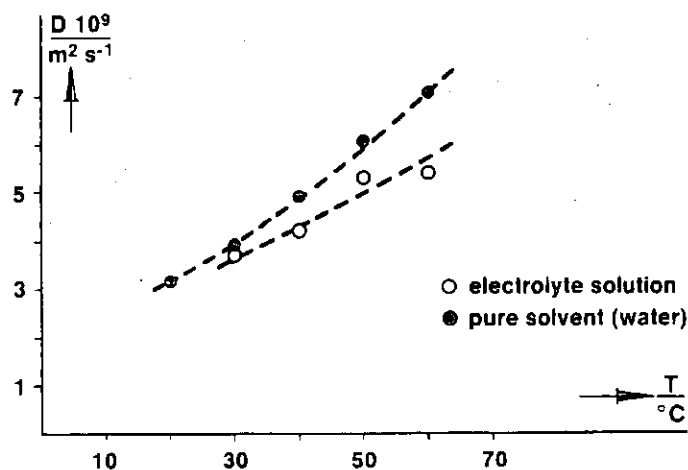


Fig. 4.7. Diffusion coefficient of hydrogen in an aqueous electrolyte solution and in the pure solvent as a function of temperature.

#### 4.6.3. Aqueous solution of 3-pentanone.

The aqueous solution contained  $100 \text{ mol m}^{-3}$  3-pentanone. Experiments were carried out at  $30 \text{ }^\circ\text{C}$ . The diffusion coefficient was calculated with the value of the Henry number ( $H_e = 0.018$ ) found from the work described in Chapter 3. The value of the diffusion coefficient determined in this way is  $3.6 \cdot 10^{-9} \text{ m}^2 \text{ s}^{-1}$ , which value is somewhat lower than that for the pure solvent. The standard deviation is  $0.4 \cdot 10^{-9} \text{ m}^2 \text{ s}^{-1}$  for 13 experiments.

#### 4.6.4. 1-Propanol.

Further experiments were carried out with the system hydrogen/1-propanol, to which in some experiments styrene was added. The concentration of styrene was  $200 \text{ mol m}^{-3}$ . All experiments were performed at  $30 \text{ }^\circ\text{C}$ .

Owing to the higher gas absorption rate, the experiments took eight minutes instead of eleven. In that time about  $1 \text{ } \mu\text{l}$  of hydrogen was absorbed into the solvent.

With a value of  $8.1 \cdot 10^{-2}$  for the Henry number the value of the diffusion coefficient found is  $8.0 \cdot 10^{-9} \text{ m}^2 \text{ s}^{-1}$ . Sporka et al. [93] reported a value of  $11.9 \cdot 10^{-9} \text{ m}^2 \text{ s}^{-1}$ , which is rather high compared with our value. However, Sporka et al. used the DRS-method, the disadvantages and unreliability of which have been pointed out in the introduction of this chapter. The addition of  $200 \text{ mol m}^{-3}$  styrene to the pure solvent did not noticeably affect the value of the diffusion coefficient. With a Henry number of  $8.1 \cdot 10^{-2}$  we calculated an experimental value of the diffusion coefficient in the solution of  $8.1 \cdot 10^{-9} \text{ m}^2 \text{ s}^{-1}$  with a standard deviation of  $0.7 \cdot 10^{-9} \text{ m}^2 \text{ s}^{-1}$  for 11 experiments.

#### 4.6.5. n-Heptane.

Owing to the high rate of gas absorption, it was necessary to use a  $5 \text{ } \mu\text{l}$  syringe for the determination of the diffusion coefficient of hydrogen in n-heptane.

First, the experiments were carried out with a syringe needle ground in the shape of a truncated cone. During these experiments it was found that the gas bubble left the tip of the needle, so that it was impossible to perform experiments in the correct way as described in section 4.4.

It seems to us that there could be three reasons for this behaviour.

- Because of the high solubility of hydrogen in n-heptane, it is possible that the surface tension gradient is influenced in such a way by the concentration gradient at the gas-liquid interface that the gas bubble leaves the tip of the needle.

We performed a number of experiments in n-heptane with different saturation levels. It appeared that even with a hydrogen concentration in the solvent of 95 % of its solubility, the gas bubble left the tip of the needle.

- Strong convection of liquid along the gas bubble could lift it from the tip of the needle. Some experiments were done with a colour tracer to see if there was any convection in the diffusion cell. However, no convection could be detected.

- Between the surface tension and the buoyancy force there exists the following relation for the gas bubble fixed at the tip of the needle:

$$(\rho_L - \rho_G)V_{bg} < \sigma d_c \pi \quad (4-29)$$

When the volume of the gas bubble is approximated by  $\pi d^3/6$ , the eqn (4-29) leads to:

$$d < \{6\sigma d_c / (\rho_L g)\}^{1/3} \quad (4-30)$$

Table 4.4. gives the calculated maximum allowable bubble diameters.

Table 4.4. Maximum allowable gas bubble diameters as calculated from eqn (4-30) for the bubble to stay fixed at the tip of the needle.

solvent	$d_{\max} \cdot 10^3 / \mu\text{m}$
water	2.1
1-propanol	1.5
n-heptane	1.5

It is obvious that in all the experiments the gas bubble diameter is smaller than the maximum allowable diameter according to Table 4.4. Another possibility is that the contact angle between gas bubble and needle in combination with the surface tension has a large influence on the fixation of the gas bubble at the tip of the needle. In Table 4.5., we have listed the values of the surface tension for water, 1-propanol and n-heptane.

Table 4.5. Values of the surface tension for water, 1-propanol and n-heptane.

solvent	$\sigma \cdot 10^3 / (\text{N m}^{-1})$
water	73
1-propanol	24
n-heptane	20

We performed a number of experiments with aqueous solutions of ethanol of different concentrations and with different values of the surface tension to see for which value of the surface tension the hydrogen gas bubble leaves the tip of the needle.

It appeared that with a concentration of about 50 vol-% ethanol the gas bubble leaves the needle. This solution has a surface tension of about  $30 \cdot 10^{-3} \text{ N m}^{-1}$ . This result is in good agreement with our experience that in n-heptane the gas bubble always leaves the tip of the needle, whereas in 1-propanol this behaviour was observed only occasionally. Apparently, for the geometry of the tip of the needle we used, the value of the surface tension at which the gas bubble leaves the needle lies somewhere between 20 and  $25 \cdot 10^{-3} \text{ N m}^{-1}$ .

To measure the diffusion coefficient of hydrogen in n-heptane we took a  $5 \mu\text{l}$  syringe with a flat-tipped needle, i.e. with  $\alpha = \pi/2$ . For the calculation of the diffusion coefficient, we made use of the value for the Henry number of  $11.5 \cdot 10^{-2}$  from the work of Wilhelm and Battino [73]. The value of the diffusion coefficient which we calculated is about  $13 \cdot 10^{-9} \text{ m}^2 \text{ s}^{-1}$ . Experiments with the same  $5 \mu\text{l}$  syringe gave however higher values for the diffusion coefficient of hydrogen in 1-propanol. Therefore, there can be some doubt about the applicability of the above-described theory for the geometry of the tip of the needle with a cone angle  $\alpha = \pi/2$ . Probably, the real value of the diffusion coefficient of hydrogen in n-heptane should be somewhat lower than  $13 \cdot 10^{-9} \text{ m}^2 \text{ s}^{-1}$ .

#### 4.6.6. Aqueous polyacrylamide solution.

In section 4.5. precautions were discussed for the determination of the diffusion coefficient according to the CBS-method.

With the CBS-method, all convection must be avoided.

If we neglect the density difference which is due to the difference in gas concentration, free convection is caused only by the temperature difference in the liquid. In the method we used, temperature differences may be caused by the light needed to project an enlarged image of the gas bubble on the screen. If the intensity of this light is too high, the liquid will be heated locally, which results in free convection of the liquid in the neighbourhood of the gas bubble. Heat transfer between two flat parallel plates is only determined by heat conduction if  $\text{Nu} = 1$ . Because for free convection  $\text{Nu} = 0.15 \text{ Ra}^{1/4}$  [94], the requirement  $\text{Nu} = 1$  is the same as the condition that

Experimentally a value of 1800 has been found for the Rayleigh number in the case of the determination of the heat conductivity of liquids in a vertical cylinder [88]. From the composition of the Rayleigh number it is clear that this number is inversely proportional to the viscosity.

In the development of the above-described CBS-method we have performed experiments to make sure that free convection is completely absent. To this end, we determined not only the diffusion coefficient of hydrogen in water but also that of hydrogen in an aqueous polymer solution at 20 and 30 °C. As polymer we used polyacrylamide (Separan AP-30 from Dow Chemical).

The advantage of the addition of polymer is that only a small amount of polymer is needed to increase the "zero-shear" viscosity enormously without changing the density of the liquid.

The aqueous polymer solutions were made according to a method described by Hamersma et al. [95].

The diffusion coefficient of hydrogen in stagnant pure water determined according to the CBS-method has a value of  $3.9 \cdot 10^{-9} \text{ m}^2 \text{ s}^{-1}$  at 30 °C and a total pressure of about 1 bar. We deliberately introduced a free convection in the liquid by increasing the light intensity. In this case we found the incorrect value of  $8.0 \cdot 10^{-9} \text{ m}^2 \text{ s}^{-1}$  for the "apparent diffusion coefficient" of hydrogen in water with free convection. With the same increased light intensity we have determined the apparent values of the diffusion coefficient of hydrogen in aqueous polymer solutions. In Fig 4.8. and Table 4.6. the results are given. It is obvious that by polymer addition free convection is fully suppressed. Further, it can be noticed that notwithstanding a large increased viscosity the value of the diffusion coefficient in the case of a completely suppressed free convection decreases only slightly ( $c_p > 500 \text{ mg kg}^{-1}$ ).

These experiments confirm that the values of the diffusion coefficient of hydrogen in water in the temperature range 20 - 60 °C and at about 1 bar total pressure were obtained from a pure diffusion process without free convection. Recently, a model has been published by Hamersma et al. [95] which shows a relation between shear-stress and shear-rate. With this model, one can calcu-

Table 4.6. Experimental values of the "apparent diffusion coefficient" of hydrogen in aqueous polymer solutions at 30 °C and about 1 bar total pressure using increased light intensity.

$c_p / (\text{mg kg}^{-1})$	$D \cdot 10^9 / (\text{m}^2 \text{ s}^{-1})$	$\sigma_D \cdot 10^9 / (\text{m}^2 \text{ s}^{-1})$	number of experiments
0	8.0*	0.3	5
50	6.4*	1.0	4
100	4.4*	0.1	4
150	4.3*	0.3	5
250	4.1*	0.3	6
500	3.8	0.2	5
1000	3.6	0.1	5
1500	3.9	0.2	5
2000	3.5	0.1	5
2500	3.6	0.2	5
5000	3.3	0.1	5
7500	3.7	0.3	5
10000	3.3	0.1	5
12500	3.7	0.2	4
15000	2.9	0.1	5
17500	3.1	0.2	5
20000	3.2	0.1	5

\* Incorrect value; correct value of the diffusion coefficient (i.e. without free convection) of hydrogen in water at 30 °C:  $3.9 \cdot 10^{-9} \text{ m}^2 \text{ s}^{-1}$



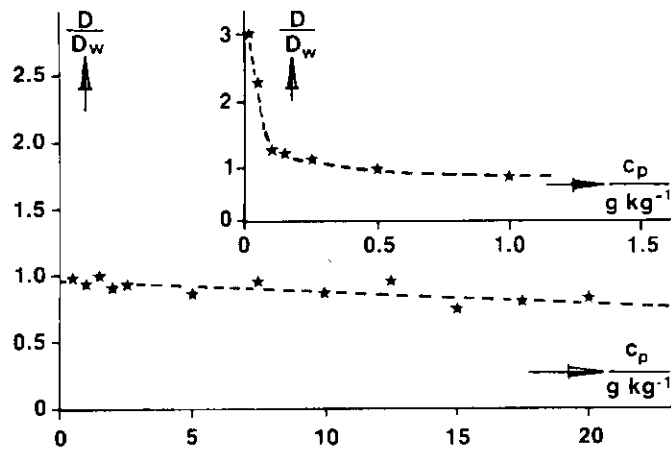


Fig. 4.8. Experimental values of the "apparent diffusion coefficient" of hydrogen in aqueous polymer solutions at 30 °C and at a total pressure of about 1 bar using increased light intensity [120].

late the values of the "zero-shear" viscosity of stagnant aqueous polymer solutions. With this knowledge we have quantitatively studied the relation between the diffusion coefficient and the "zero-shear" viscosity of these aqueous polymer solutions at 20 °C and at about 1 bar total pressure. In Fig. 4.9. and Table 4.7. the results of this study are given. Again a small decrease of the value of the diffusion coefficient with increasing "zero-shear" viscosity is found. It must be pointed out that for the calculation of the diffusion coefficient in diluted aqueous polymer solutions the same Henry number has been used as has been done for the calculation of the diffusion coefficient in pure water.

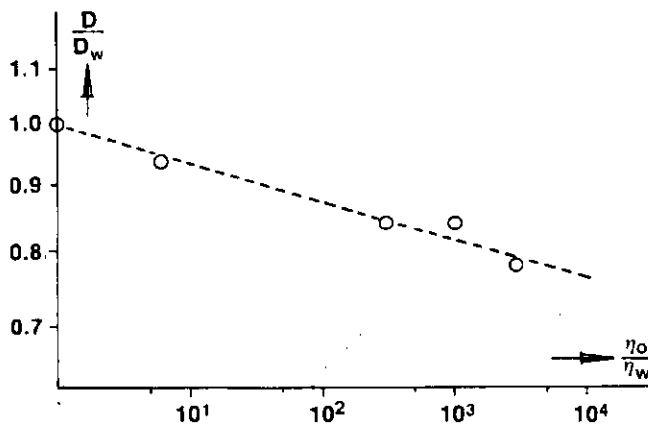


Fig. 4.9. Experimental values of the diffusion coefficient of hydrogen in aqueous polymer solutions as a function of the "zero-shear" viscosity at 20 °C and at about 1 bar total pressure [120].

Table 4.7. Experimental values of the diffusion coefficient of hydrogen in aqueous polymer solutions as a function of the "zero-shear" viscosity at 20 °C and at about 1 bar total pressure.

$c_p / (\text{mg kg}^{-1})$	$\eta_0 \cdot 10^3 / (\text{Pa s})$	$D \cdot 10^9 / (\text{m}^2 \text{ s}^{-1})$	$\sigma_D \cdot 10^9 / (\text{m}^2 \text{ s}^{-1})$	number of experiments
0	1.00	3.2	0.2	13
50	6.0	3.0	0.1	5
1000	305	2.7	0.1	6
2500	1020	2.7	0.1	5
5000	2940	2.5	0.1	6

#### 4.7. Absorption of helium in water.

Although not of primary interest for the hydrogenation reactions, further experiments were carried out with the system helium-water in the temperature range 20 - 60 °C. The procedure followed was the same as for all other systems. In Fig. 4.10. and Table 4.8. the results of these experiments are given. The diffusion coefficients have been calculated with the values of the Henry number given by Wilhelm, Battino and Wilcock [74].

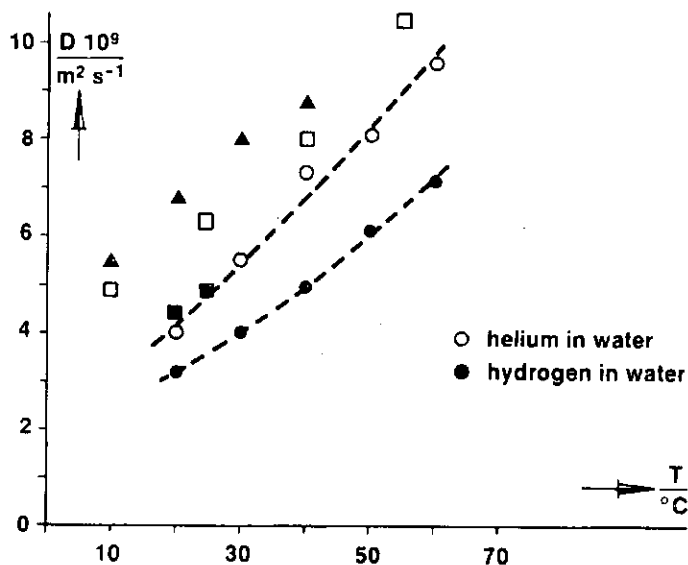


Fig. 4.10. Experimental values of the diffusion coefficient of helium in water at about 1 bar total pressure. ■ Gertz and Loeschke [96], ▲ Wise and Houghton [87], □ Ferrell and Himmelblau [89], ○ ● present work.

Table 4.8. Experimental values of the diffusion coefficient of helium in water at about 1 bar total pressure in the temperature range 20 - 60 °C.

T/°C	$D \cdot 10^9 / (\text{m}^2 \text{ s}^{-1})$	$\sigma_D \cdot 10^9 / (\text{m}^2 \text{ s}^{-1})$	number of experiments
20	4.0	0.2	10
30	5.5	0.5	10
40	7.3	0.5	10
50	8.1	0.5	10
60	9.6	0.5	10

From Fig. 4.10. it can be concluded that our experimental values in the range 20 - 30 °C are in good agreement with the results from Gertz and Loeschke at 20 and 25 °C [96].

Most experiments have been performed at room temperature. Only Wise and Houghton [87] and Ferrell and Himmelblau [89] have determined values for the diffusion coefficient in the temperature range 20 - 60 °C.

As in the case of the hydrogen-water system, most values from the literature are higher compared with the experimental results we obtained. In section 4.6.1. the reason for this difference has already been explained in detail.

#### 4.8. Predicting equations.

No less important for chemical engineering practice is the comparison of our experimental results with the values predicted by several semi-empirical relationships from the literature. Not only to find an agreement between our values and those predicted by these equations, but rather to be able to test these relationships as to their exactness. So, the diffusion coefficient can be predicted with more accuracy and reliability at different temperatures, even for other gas-liquid systems.

The temperature dependence of the diffusion coefficient will first be correlated by the Stokes-Einstein equation, developed as early as 1905 [97]:

$$D_{AB} = kT / (6\pi\eta_B R_A) \quad (4-32)$$

More recent correlations have been proposed by Wilke and Chang [98], Othmer and Thakar [99] and Scheibel [100]:

$$\text{Wilke and Chang: } D_{AB} = C_9 kT (\chi \tilde{M}_B)^{1/2} / (\eta_B \tilde{V}_A^{0.6}) \quad (4-33)$$

$$\text{with } C_9 = 42.6 \cdot 10^5 \text{ m}^{0.8} \text{ kg}^{-0.5} \text{ mol}^{-0.1} \quad (4-34)$$

Othmer and Thakar: for water as solvent:

$$D_{AB} = C_{10} / (\eta_w^{1.1} \tilde{V}_A^{0.6}) \quad (4-35)$$

$$\text{with } C_{10} = 17.6 \cdot 10^{-16} \text{ m}^{2.7} \text{ kg}^{1.1} \text{ mol}^{-0.6} \text{ s}^{-2.1} \quad (4-36)$$

for other solvents:

$$D_{AB} = C_{11} / \{ \tilde{V}_A^{0.6} \eta_B (10^3 \eta_w)^{1.1 (\Delta H_{\text{vap},B} / \Delta H_{\text{vap},w})} \} \quad (4-37)$$

$$\text{with } C_{11} = 35.2 \cdot 10^{-16} \quad (4-38)$$

$$\text{Scheibel: } D_{AB} = C_{12} kT / (\eta_B \tilde{V}_A^{1/3}) \quad (4-39)$$

$$\text{with } C_{12} = (59.4 \cdot 10^5) \{ 1 + (3\tilde{V}_B / \tilde{V}_A)^{2/3} \} \text{ mol}^{-1/3} \quad (4-40)$$

for water as solvent, if  $\tilde{V}_A < \tilde{V}_B$ :

$$C_{12} = 18.3 \cdot 10^6 \text{ mol}^{-1/3} \quad (4-41)$$

for benzene as solvent, if  $\tilde{V}_A < 2\tilde{V}_B$ :

$$C_{12} = 13.7 \cdot 10^6 \text{ mol}^{-1/3} \quad (4-42)$$

for other solvent, if  $\tilde{V}_A < 2.5\tilde{V}_B$ :

$$C_{12} = 12.7 \cdot 10^6 \text{ mol}^{-1/3} \quad (4-43)$$

$\chi$  is the so-called association parameter of the solvent, which is 2.6 for water, 1.9 for methanol, 1.5 for ethanol and 1.0 for unassociated liquids.